An integrative model of Parkinson's disease treatment including levodopa pharmacokinetics, dopamine kinetics, basal ganglia neurotransmission and motor action throughout disease progression

Noname manuscript No.
(will be inserted by the editor)

An Integrative Model of Parkinson's Disease Treatment Including Levodopa Pharmacokinetics, Dopamine Kinetics, Basal Ganglia Neurotransmission and Motor Action throughout Disease Progression

Florence Véronneau-Veilleux · Philippe Robaey · Mauro Ursino · Fahima Nekka

Received: date / Accepted: date

Abstract Levodopa is considered the gold standard treatment of Parkinson's disease. Although very effective in alleviating symptoms at their onset, its chronic use with the progressive neuronal denervation in the basal ganglia leads to a decrease in levodopa's effect duration and to the appearance of motor complications. This evolution challenges the establishment of optimal regimens to manage the symptoms as the disease progresses. Based on up-to-date pathophysiological and pharmacological knowledge, we developed an integrative model for Parkinson's disease to evaluate motor function in response to levodopa treatment as the disease progresses. We combined a pharmacokinetic model of levodopa to a model of dopamine's kinetics and a neurocomputational model of basal ganglia. The parameter values were either measured directly or estimated from human and animal data. The concentrations and behaviors predicted by our model were compared to available information and data. Using this model, we were able to predict levodopa plasma concentration, its

F. Véronneau-Veilleux
Faculté de Pharmacie, Université de Montréal,
Montréal, Québec, Canada
E-mail: florence.veronneau-veilleux@umontreal.ca

M. Ursino
Department of Electrical, Electronic and Information Engineering Guglielmo Marconi, University of Bologna
40136 Bologna, Italy

P. Robaey
Faculty of Medicine, University of Ottawa,
Ottawa, Ontario, Canada

F. Nekka
Faculté de Pharmacie, Université de Montréal,
Centre de recherches mathématiques, Université de Montréal,
Centre for Applied Mathematics in Bioscience and Medicine (CAMBAM), McGill University
Montréal, Québec, Canada

related dopamine concentration in the brain and the response performance of a motor task for different stages of disease.

Keywords Parkinson's disease · Levodopa · Dopamine kinetics · Basal ganglia · Denervation

1 Introduction

Parkinson's disease is the second most common neurodegenerative disorder after Alzheimer's [68]. Its generated motor symptoms are associated with the loss of dopaminergic neurons in the substantia nigra in the nigrostriatal pathway [68], leading to dopamine depletion in the striatum (caudate putamen). Symptoms of Parkinson's disease include rigidity, tremor at rest, postural disabilities, and bradykinesia, which is a disabling symptom defined by the slowness of the movements. The complexity of the disease and its involved mechanisms calls for the development of an integrative approach using mathematical modeling.

Going beyond a descriptive role, the main objective of the current study is to develop a holistic approach that integrates a mechanistic model of basal ganglia, levodopa kinetics and dopamine kinetics in order to help understanding the underlying mechanisms of Parkinson therapy as the disease progresses and to design proper therapeutic interventions. With this objective in mind, we put within the same framework a pharmacokinetic (PK) model of levodopa that we interface with a neurocomputational model of basal ganglia, where dopamine kinetics is mechanistically described. The temporal profiles of levodopa concentration in plasma and brain, as well as dopamine concentration in the brain are derived. The model presented here could be used in future studies to optimize levodopa's regimen in an individualized manner.

To assess the degree of severity of the disease, numerous tests are used and expressed in different scales, the most common being the Unified Parkinson's Disease Rating Scale (UPDRS). The finger tapping task is generally used as a clinical biomarker since it has been shown to correlate with bradykinesia subscore in terms of UPDRS scale [43, 72]. The tapping frequency was used here as an output of the model to study the motor activity of patients and the severity of bradykinesia.

Levodopa, considered as a gold standard treatment, is one of the most effective drugs to relieve motor symptoms of Parkinson's disease [55]. While levodopa appears to slow disease progression [42] and to have long duration response [16], it does not completely stop the progression of denervation [64]. Denervation is therefore an important aspect of the present work. Levodopa is converted to dopamine and acts in reducing the disease symptoms[19]. Unfortunately, while levodopa is very effective during the first years of therapy, its effect is altered with the progression of the disease. The initial period of long-lasting effect with almost complete suppression of symptoms is referred to as the "honeymoon period" [41]. After several years of treatment, the effect duration and the delay between plasma concentration and effect shorten

Update A

[41], leading to more frequent administration of levodopa and higher doses. This is thought to induce disabling side effects such as involuntary movements called dyskinesias [70]. These complications call for a better understanding of the modification of the mechanisms involved in disease progression and the response to therapy.

The integrative model developed here presents three novelties. First, our model takes into account levodopa's, dopamine's and basal ganglia's kinetics all together with physiologically interpretable parameters. Second, the effect of nigrostriatal denervation throughout the model is represented. Finally, each model component is separately verified through comparison with available data, providing reliability of its predictions. Altogether, this leads to an integrative and physiologically realistic model that helps understanding Parkinson's disease's progression and its medication.

Previous studies have looked separately at the effect of levodopa, the dopamine kinetics and the neurotransmission in the basal ganglia.

The evolution of the therapeutic effect of levodopa during the progression of the disease was previously evaluated using empirical equations, namely the E_{max} models [15,18,41,54,74]. Disease progression was correlated with pharmacodynamic parameters and levodopa duration effect [74]. Studies were conducted to assess the difference in the pharmacodynamic parameters between early and advanced parkinsonian patients. Modifications in parameters such as endogenous effect of dopamine [15], endogenous release [41], maximal change in response [15], maximal effect [41], concentration to 50% effect (EC_{50}) [18] and steepness of effect curve [74] were observed. Although these studies highlight the importance of incorporating disease progression into pharmacodynamic modeling of levodopa, they do not provide mechanistic explanation. In the current work, the influence of disease progression on release, recapture and elimination of dopamine in the brain is explicitly modeled to enable a better understanding of the evolution of levodopa's effects with the disease.

Previous studies focused exclusively on the modeling of dopamine kinetics with and without levodopa in Parkinson's disease [9,25,26,60,61]. Although more complex and detailed, these models did not include the effect of dopamine on the basal ganglia. Since dopamine concentration does not invariably reflect the effect of levodopa throughout the disease, it was important to include the neuronal activity in the model. Other models were more concerned with dopamine kinetics in normal and pathological states and did not address therapy [9,25,26]. Compared to these models, the use of the present model can be extended to understand the impact of different mechanisms (such as modification of receptor's density, of DATs recapture, of neurotransmission,...) on the disease progression and its medication.

Other studies have focused their work on understanding Parkinson's disease through neurocomputational models of basal ganglia, which is the extrapyramidal center of control, selection and initiation of movement [5,7,6,14, 21,28,37,29,35,50,65,75,78]. Basal ganglia are composed of subregions and include the striatum, the globus pallidus, the substantia nigra and subthalamic nucleus. The neurotransmission is carried out through the direct, the indirect

and the hyperdirect striatal output, where the former promotes the movement, the second decreases it, and the latter is responsible for suppression of erroneous movements. In the classical models [3,20,22], a proper action selection is thought to be the result of a balance between these pathways. Dopamine (DA) loss involved in Parkinson's disease is reported to disrupt this natural balance at the striatal level [3]. Although the above mentionned model of basal ganglia included the nuclei and the neurotransmission pathways, neither of them included dopamine kinetics as ours.

The current study focuses on the modeling of levodopa and its effect on both dopamine kinetics and basal ganglia function through a quantitative systems pharmacology approach. It is aimed to provide a more thorough understanding of levodopa kinetics and action. The model here developed tries to keep a good balance between simplicity and accuracy. The paper is organized as follows. The description of the three submodels and the role of neuronal death in the evolution of the different involved mechanisms are given in Section 2. The validation of the whole model using available data is presented in Section 3.1. Simulation of a virtual patient and the effect of the progression of the disease on the motor task are presented in section 3.2 and 3.3 respectively. Details on the model and the scaling of some equations are given in the Supplementary material.

2 Methods

The whole model is divided into three parts, each of which is detailed in a separate section below. It represents the different mechanisms relevant to understand the effect of levodopa and the progression of the disease on dopamine kinetics and neurotransmission in the basal ganglia. This physiological integrative model is a combination and an extension of three models previously proposed [6,7,25]. The first part consists in a pharmacokinetic model of levodopa, adapted from Baston et al. [6]. The dopamine kinetics model is detailed in the second part. The processes of dopamine's release, recapture by dopamine transporters (DATs), elimination and occupancy of the dopaminergic receptors are included, along with their interrelationship with nigrostriatal denervation. In the third part, the neuronal activity of each region of the basal ganglia is reproduced by simulating the direct, indirect and hyperdirect neurotransmission pathways and their response to dopamine concentrations. The finger tapping frequency as an output of the integral model is assessed. Figure 1 depicts the three models and their connections.

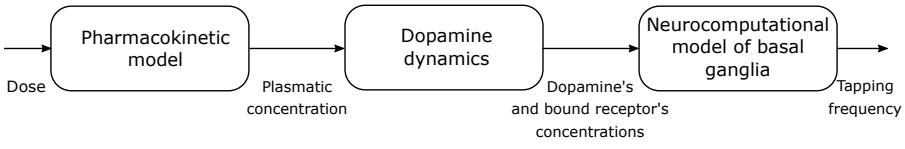

Fig. 1 Representation of the three parts of the whole model

Disease progression is represented here by the degree of nigrostriatal denervation, described with the fraction of neurons alive in the substantia nigra, noted f, which alters the mechanisms involved in the three different parts of the model. When a linear regression between the neural density and the UPDRS3 score was performed [33], it was shown that neuronal density in the substantia nigra is inversely correlated with UPDRS3 score [33], so would be the case for the fraction f.

2.1 Modeling the pharmacokinetics of levodopa

The dopamine precursor levodopa is one of the most effective treatments of Parkinson's disease. Unlike dopamine, it is able to cross the blood brain barrier to reach the basal ganglia. Levodopa is then decarboxylated into dopamine by the neurons of the substantia nigra, enhancing dopamine release by the remaining dopaminergic neurons. Levodopa has been shown to successfully alleviate symptoms for many years following the initial diagnosis. With disease progression, the effect duration and the delay in the effect are thought to be shorter because of the loss of buffering capacity of the neurons [27,56,59]. In early stages of the disease, the neurons, which are still in sufficient quantity, store dopamine and release it into the synaptic cleft as required. This allows the effect of levodopa to last longer than its plasma concentration. With the progression of the disease and the loss of dopaminergic neurons, this storage capacity is presumably lost and dopamine is released almost immediately. At this stage, levodopa effect starts to mimic the plasma concentration. Pharmacodynamics studies using an E_{max} model have shown an increase in EC_{50} and the Hill coefficient N with progression of the disease measured by Hoehn and Yahr (H&Y) stages [1,18]. This increase in pharmacodynamic parameters with disease progression is however still subject to debate [16]. It does not however concern the model developed in this work because the E_{max} model is substituted by a dopamine kinetics model combined to a neurocomputational model of basal ganglia. The dopamine kinetics model is used to represent the different processes regulating dopamine concentration in the striatum (release, recapture and removal). This model is linked to a neurocomputational model to represent the dopamine action on the neurotransmission pathways.

Update B

Pharmacokinetic (PK) studies [6,15,67] have shown that two-compartment models are good fit of levodopa concentrations. The herein PK model was adapted from [6], which was used with the neurocomputational model of basal ganglia to represent the PK of a typical patient. Figure 2 is a schematic representation of the PK model.

Concentrations C_1 and C_2 in the central and peripheral compartments are respectively given by:

$$V_1 \frac{dC_1}{dt} = k_0(t) + Q_{21}C_2 - (Q_{12} + CL_{etot})C_1, \tag{1}$$

$$V_2 \frac{dC_2}{dt} = Q_{12}C_1 - Q_{21}C_2, \tag{2}$$

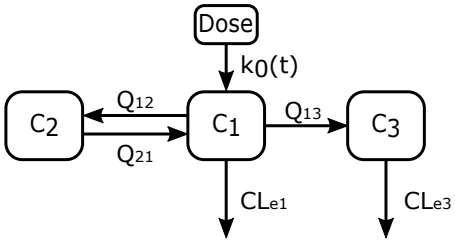

Fig. 2 Representation of the two compartment pharmacokinetic model of levodopa with a third compartment for levodopa in the brain

where Q_{ij} is the inter-compartment clearance between the ith and the jth compartments. As mentioned in [6], Q_{12} and Q_{21} take slightly different values to provide good fitting of individual plasma concentrations. This raises a problem of identifiability of parameters Q_{12} and Q_{21} that was not addressed in the present work. The total clearance is given by the parameter CL_{etot} with $CL_{etot} = CL_{e1} + Q_{13}$. The infusion rate is $k_0(t)$. As the disease progresses, the PK of levodopa remains the same, so the parameters of equations 1 and 2 are not affected by the fraction f of neurons alive [18]. Levodopa brain concentrations in the third compartment C_3 are given by:

Update C

$$V_3 \frac{dC_3}{dt} = Q_{13}C_1 - CL_{e3}C_3. \tag{3}$$

At early stages of the disease, dopamine is still functionally released in the synaptic cleft, modulated by the need in dopamine. With disease progression, this buffering effect of the neurons is increasingly lost, leading to a rapid and pulsatile rather than continuous release of dopamine in the synaptic cleft [73]. This loss of buffering effect was previously modeled by assuming that the value of CL_{e3} is increased with the loss in dopamine [18,38,54,53,74]. The parameter CL_{e3} which represents the clearance from the effect compartment (here the brain) was shown to be correlated with nigrostriatal denervation [24]. Parameter Q_{13} was also previously correlated with denervation [11,18,76]. In the current model, we assumed that both CL_{e3} and Q_{13} are correlated with the loss of neurons. Indeed, since dopamine is released more rapidly due to the loss of buffering capacity in the synaptic cleft, Q_{13} is assumed to become higher with denervation. It is as if levodopa fills a reservoir that slowly leaks and becomes leakier with denervation, hence CL_{e3} and Q_{13} are higher with denervation. With the progression of the disease, equation 3 is modified and the concentration in the brain is given by:

$$V_3 \frac{dC_3}{dt} = \frac{1}{f} \cdot Q_{13}C_1 - \frac{1}{f} \cdot CL_{e3}C_3. \tag{4}$$

The denervation progresses with disease, resulting in a smaller fraction f of neurons alive (higher values of $1/f$.)
The value of parameter CL_{e1} is much larger than the value of Q_{13}, hence the value of CL_{etot} is almost equal to CL_{e1}. For the sake of simplicity, the

total elimination parameter ($CL_{etot} = CL_{e1} + Q_{13}$) of the first compartment has been maintained constant throughout the disease even if Q_{13} is modifed by f. This choice is supported by the observation that denervation does not impair the pharmacokinetics, hence the total elimination remains unchanged [18]. Most parameter values were taken from patient 1 in [6], estimated from plasma concentrations and effect (measured as finger tapping frequency) by considering $f = 0.30$. Only parameter Q_{13} was estimated to obtain a maximal levodopa brain concentration close to the one presented in [52]. Patient 1 was chosen since he exhibits quite a stable response to levodopa, with just a moderate decrease in tapping frequency during the first hours after drug administration. The behavior of more unstable patients presented in [6] can be simulated via a reduction in f, as demonstrated below. No significant difference was seen in pharmacokinetics between patients with or without motor fluctuations in previous studies [6,27,54]. The parameter values are presented in Table 1.

Update D

Table 1 Parameter values of the PK model

Parameter	Description	Value	Reference
Q_{12}	Inter-compartmental clearance from compartment 1 to 2	9.11 L/min*	[6]
Q_{21}	Inter-compartmental clearance from compartment 2 to 1	10 L/min*	[6]
Q_{13}	Inter-compartmental clearance from compartment 1 to 3	0.0021 L/min	estimated
CL_{e3}	Clearance from compartment 3	0.006 L/min	[6]
CL_{e1}	Clearance from compartment 1	0.7979 L/min	[6]
V_1	Volume of compartment 1	12 L	[6]
V_2	Volume of compartment 2	32 L	[6]
V_3	Volume of compartment 3	2 L	[6]
$k_0(t)$	Infusion rate	3.33 mg/min for $0 \leq t \leq 30$min 0 mg/min for $t \geq 30$min	[6]

Update D

* The values of Q_{12} and Q_{21} are not identifiably different.

2.2 Modeling the Dopamine Kinetics

The extracellular dopamine concentration in the striatum is regulated by different processes. It is synthesized by dopaminergic neurons of the substantia nigra and released in the striatum. It can then be recaptured by DATs on the presynaptic neurons and eliminated or removed from the synaptic cleft. The remaining dopamine molecules can bind to dopaminergic receptors (D1 and D2 receptors are considered here) on the postsynaptic neurons. To maintain

simplicity of the model, not all reactions in the neurons nor interactions with enzymes are detailed, but only the main processes for which information and data are accessible. Indeed, dopamine metabolism and DAT density were evaluated through both positron emission tomography (PET) and single-photon emission computed tomography (SPECT) [34]. Distruption in the L-Tyrosine to vesicular dopamine pathway was not modeled here as in [61]. Focus was kept on release, reuptake and elimination of dopamine in the synaptic cleft and their influence on dopamine concentration.

Figure 3 illustrates the processes of dopamine kinetics included in the model.

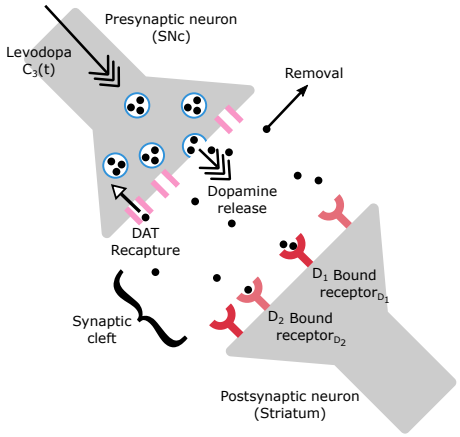

Fig. 3 Schematic representation of release, recapture by DATs, binding to receptors and elimination of the dopamine in the synaptic space.

We here explicitly add the influence of removal that can be affected in different ways by the loss of dopaminergic neurons. The processes of release, recapture and elimination were described in the current model using the following relation to express dopamine concentration $C_{dop}(t)$ in μMole/L in the synaptic space:

$$\underbrace{V_{SC}\frac{dC_{dop}(t)}{dt}}_{\text{Dopamine concentration}} = \underbrace{\tilde{I}_{DA}(t)}_{\text{Dopamine Release}} - \underbrace{\frac{\tilde{V}_{max}C_{dop}(t)}{(k_m + C_{dop}(t))}}_{\text{Recapture by DATs}} - \underbrace{CL_{rem}C_{dop}(t)}_{\text{Removal}} \quad (5)$$

where V_{SC} is the volume of the synaptic cleft. It is possible to rewrite equation 5 as the following:

$$\frac{dC_{dop}}{dt} = \frac{\tilde{I}_{DA}(t)}{V_{SC}} - \frac{\tilde{V}_{max}C_{dop}(t)}{V_{SC}(k_m + C_{dop}(t))} - \frac{CL_{rem}}{V_{SC}}C_{dop}(t) \quad (6)$$

$$= I_{DA}(t) - \frac{V_{max}C_{dop}(t)}{k_m + C_{dop}(t)} - k_{rem}C_{dop}(t) \quad (7)$$

where the values of parameters V_{max}, k_m and k_{rem} are given in Table 2. The binding of dopamine to receptors was neglected in equation 5 as in [44] because dopamine kinetics are dominated by transporters uptake rather than by binding to receptors. Indeed, the removal of dopamine from synaptic cleft by receptors binding is much slower than from reuptake by transporters DATs [44]. The variable $I_{DA}(t)$ could account for dopamine release from serotoninergic terminals in future studies. In the current study, $I_{DA}(t)$ only expresses release by dopaminergic neurons. The details of the determination of the variable $I_{DA}(t)$ are presented in Section S.2 of the Supplementary Material. This release variable is the sum of the endogenous dopamine produced by L-Dopa decarboxylation and the exogenous dopamine produced by levodopa decarboxylation. In the present model, levodopa brain concentration needs to be converted into its equivalent increase in dopamine release. Exogenous dopamine release by levodopa is assumed to be proportionnal to concentration C_3:

$$I_{DA}(t) = I_{DAendogenous} + I_{DAlevodopa}(t) \tag{8}$$
$$= I_{DAendogenous} + k_{3dop}C_3(t). \tag{9}$$

The value of $I_{DAendogenous}$ is given in Table 2. $I_{DAendogenous}$ is considered to be the constant tonic release of dopamine and $I_{DAlevodopa}$ is changing in time as concentration of levodopa in the brain C_3 is changing. $I_{DAendogenous}$ and $I_{DAlevodopa}$ are proportional to the terminal density, the vesicular release probability, the number of molecules released per vesicule fusion and the average firing rate of dopaminergic neurons. They are inversely proportional to the extracellular volume fraction and the Avogadro's constant [25]. The parameter k_{3dop} also contains the conversion factor of C_3 from $\mu g/mL$ to $\mu mol/L$. More details are given in section S.2 of Supplementary material. The scaling of levodopa brain concentration into its related release of dopamine is presented in section S.1 of Supplementary material. Recapture by DATs is a saturable process given by a Michaelis-Menten equation. All other processes leading to the removal of dopamine such as diffusion far from the release site, or metabolism by the Catechol-O-methyltransferase (COMT) in glial cells or neurons, are considered linear [13,25]. Equation 7 was proposed in several papers dedicated to dopamine kinetics [9,25,60]. The merit of this equation lies in the physiological interpretation of its involved parameters, readily measurable from experimental data.

As the disease progresses, neurons will die in the substantia nigra, leading to changes in the dopamine kinetics. Considering f as the fraction of neurons alive, equation 5 becomes:

$$\frac{dC_{dop}(t)}{dt} = f \cdot I_{DA}(t) - \frac{f \cdot V_{max}C_{dop}(t)}{(k_m + C_{dop}(t))} - \frac{1}{f} \cdot k_{rem}C_{dop}(t). \tag{10}$$

It is assumed that the release variable $I_{DA}(t)$ decreases linearly with the loss of neurons. While the exact relation is not known, the recapture by DATs is also assumed to decrease linearly with the loss of neurons in the present model since the transporters are located on the dying neurons [25,60]. The linear removal

from the synaptic cleft is usually lower compared to reuptake because the neurons of the substantia nigra are densely packed, so the dopamine molecules are recaptured by DATs from neighboring terminals before they have had time to be removed by other mechanisms. As the disease progresses and the terminals become sparser, it gets easier for the dopamine molecules to be removed, justifying the assumption of inverse proportionality to the fraction of neurons alive for linear removal [60]. As shown in Figure 4, the main route of dopamine elimination from the synaptic cleft is through recapture by DATs until too many neurons have died. The contribution of enzymatic elimination or of the other removal processes increases with denervation and it becomes the dominant one when $f < 0.05$.

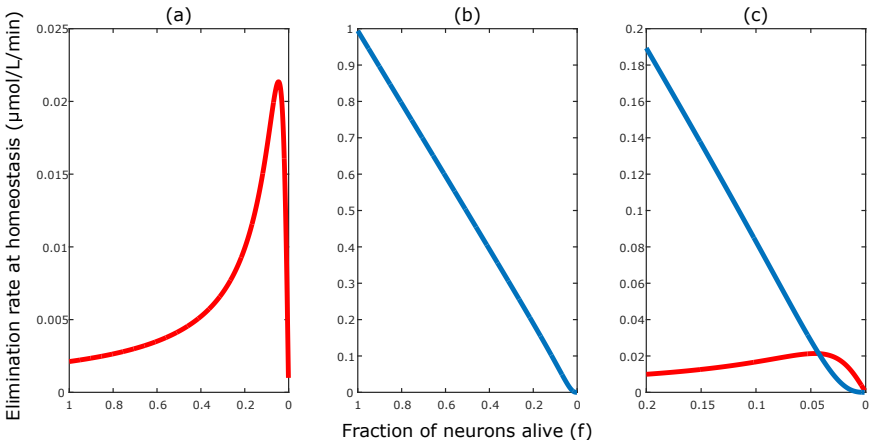

Fig. 4 (a) Rate of dopamine linear removal at homeostasis, (b) Rate of dopamine's recapture by DATs transporters at homeostasis and as function of fraction of neurons alive (f) (c) Both recapture and removal routes for f below 0.2

Once in the synaptic cleft, dopamine can bind to dopaminergic receptors D1 and D2. The concentration of bound receptors to dopamine of type i with $i \in \{D1, D2\}$ is given by the following equation:

$$\text{Bound receptor}_i = \frac{B^i_{max} C_{dop}}{k^i_D + C_{dop}}. \tag{11}$$

The maximal concentration of receptors of type i is given by B^i_{max}. The dissociation constant k^i_D of the receptors changes according to receptors' affinity. k^i_D is approximatively 1 μM for low affinity state and 0.01 μM for high affinity state [51,62]. In the striatum, we considered that most of the $D1$ receptors are in low affinity state and $D2$ receptors are in high affinity state [62]. The parameter values of equations 7 and 11 are given in Table 2 with the references from which they were drawn. The bound receptor concentration will be considered representative of the postsynaptic effect of dopamine [39]. In the neurocomputational model of basal ganglia, Bound receptorD_1 and Bound receptorD_2

Table 2 Parameter values for the dopamine kinetics model

Parameter	Descrition	Value	Reference
$I_{DAendogenous}$	Endogenous release rate	0.9963 μmol/L/s	[25]
V_{max}	Maximal reuptake rate by DATs	4 μmol/L/s	[25]
k_m	DATs dissociation constant	0.16 μmol/L	[25,60]
k_{rem}	Removal rate	0.04 1/s	[13,25]
k_D^{D1}	D1 receptor dissociation constant	1 μmol/L	[48]
k_D^{D2}	D2 receptor dissociation constant	0.01 μmol/L	[48]
B_{max}^{D1}	D1 receptor maximal density	0.007 μmol/L	[17]
B_{max}^{D2}	D2 receptor maximal density	0.015 μmol/L	[45]

act on the activity of neurons in the striatum. Bound receptorD_1 acts on the Go pathway and Bound receptorD_2 on the NoGo and cholinergic pathways.

2.3 Modeling the Basal Ganglia

The basal ganglia are the control center for movement's selection and initiation [49]. They are composed of subcortical nuclei such as the striatum, the globus pallidus, the substantia nigra and the subthalamic nucleus. They are divided in three main neurotransmission pathways: the direct pathway which promotes the movement, the indirect pathway which decreases the movement and the hyperdirect pathway which suppresses erroneous movement. The direct pathway connects the striatum, the globus pallidus internal (GPi) and the thalamus. The indirect pathway connects the striatum, the globus pallidus external (GPe), the GPi and the thalamus. The dopaminergic receptors present on the neurons of the striatum are mainly D1 (Go or G) and D2 (NoGo or N). Neurons presenting D1 and D2 receptors will be considered separately in the model since direct-pathway striatal neurons contain more D1 receptors, while indirect-pathway striatal neurons contain more D2 receptors [30]. Finally, the hyperdirect pathway connects the cortex to the subthalamic nucleus. In the classical model [3,20,22], correct motor responses are the result of balance between these three neurotransmission pathways. This classical model states that, in Parkinson's disease, this balance is lost. Dopamine acts on the neurotransmission pathways. It is mainly excitatory for D1 and inhibitory for D2. In the current model, dopamine also acts on the striatal cholinergic interneurons. In this model, dopamine inhibits cholinergic interneurons, which in turn provides inhibition to the Go neurons and excitation to the NoGo neurons, with an opposing role compared with dopamine. The thalamus and cortex are also included in the current model to complete the neurotransmission loop. A schematic representation of the basal ganglia nuclei and the three neurotransmission pathways of the model is given in Figure 5.

The neurocomputational model of basal ganglia was previously developed to investigate the motor function in the finger tapping task [6,7]. Each subcortical nuclei of the basal ganglia is divided in two "neurons" to represent the two binary actions of the task: rising the finger and lowering the finger. Firing

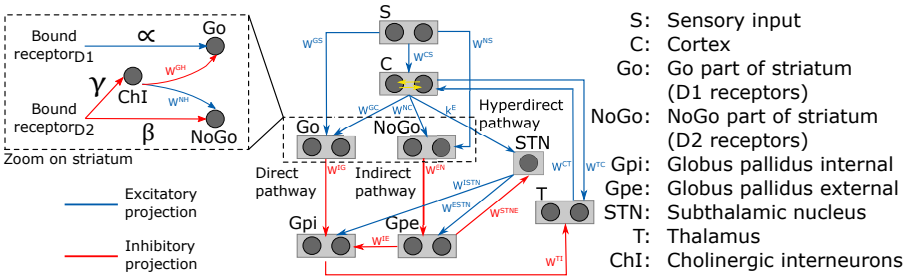

Fig. 5 Schematic representation of the basal ganglia and the three neurotransmission pathways [6]

rate type equations were used to represent the neural activity in each region. The equations and details of this model are presented in Section S.3 of the Supplementary material. In the neurocomputational model of basal ganglia, Bound receptor$_{D1}$ and Bound receptor$_{D2}$ act on the activity of neurons in the striatum. In particular, Bound receptor$_{D1}$ excites activity of the Go pathway and Bound receptor$_{D2}$ excites activity of the NoGo one. Moreover, Bound receptor$_{D2}$ acts on the cholinergic system which, in turn, amplifies the effect of the dopaminergic term. As a consequence, a dopamine increase activates the Go pathway, favoring action selection, while a decrease in dopamine activates the NoGo pathway, preventing action selection. The finger tapping task was simulated as a choice between two actions (finger down, finger up) which are alternatively given as input to the model. At the end of each action, before starting the new one, a time lag of 115 ms is inserted [6], to simulate the time necessary to perform the action. Hence, the tapping frequency depends on the balance between the Go, NoGo and cholinergic pathways, which, in turn, are a function of bound receptors.

2.4 Connecting the three submodels

The plasma concentration of levodopa is given by the pharmacokinetic model. Once it crosses the blood brain barrier, levodopa is decarboxylated into dopamine by the neurons of the substantia nigra. The release of exogenous dopamine will be added to the endogenous one. Indeed, the release term $I_{DA}(t)$ is the sum of the endogenous and exogenous dopamine, which is related to the concentration in the third compartment $C_3(t)$. Dopamine will then bind to receptors D_1 and D_2. Its post-synaptic effect will be given by the concentration of bound receptors through the parameters Bound ReceptorD_1 and Bound ReceptorD_2, respectively. These parameters will affect the neurotransmission in the basal ganglia nuclei and thus will modify the final motor response. Dopamine and levodopa concentrations, both in plasma and brain, are given in $\mu mol/L$ and $\mu g/mL$, respectively. Their equivalent concentrations in different units could be obtained by considering dopamine's molar mass at $153,18\ g/mol$ and lev-

Update E

odopa's molar mass at 197, 1879 g/mol. Figure 6 is a schematic representation of the whole model with the connections between the three submodels.

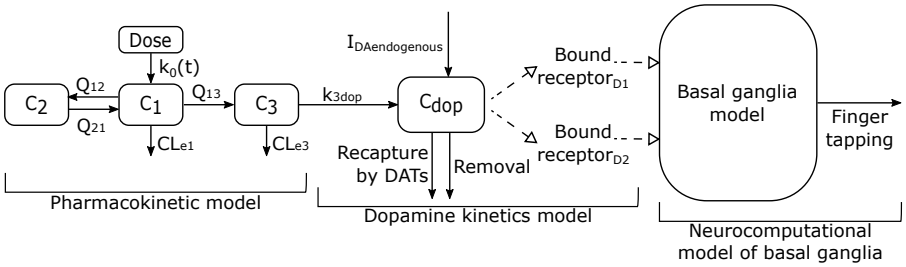

Fig. 6 Schematic representation of the three submodels connected

All simulations were performed with Matlab R2018a using standard libraries.

3 Results

The processes involved in the progression of Parkinson's disease and the effect of levodopa are not still fully understood. The current model is based on the up-to-date pathophysiological and pharmacological knowledge. Several physiological parameters were measured either in animals or humans. The parameters of the neurocomputational model of basal ganglia were previously fitted [6] to tapping frequency data recorded 12 times over 200 minutes for a group of six patients.

3.1 Representation of physiological data

In the following, the output of each submodel was either compared with available physiological data or to well-documented behaviour.

3.1.1 PK model

Pharmacokinetic parameters previously fitted to data taken from patient 1 in this study [6] were used here. This patient received 100 mg of levodopa. The PK parameters were estimated to fit the data of nine samples over a 200-minutes period.

Levodopa concentration in the basal ganglia is given by the concentration in the third compartment of the PK model (C_3). This concentration has been measured in humans by microdialysis [52]. Using our model, we simulated the maximal levodopa concentration in the brain as ~ 1 μmol/L, which is close to the one measured in humans (~ 0.8 μmol/L) [52].

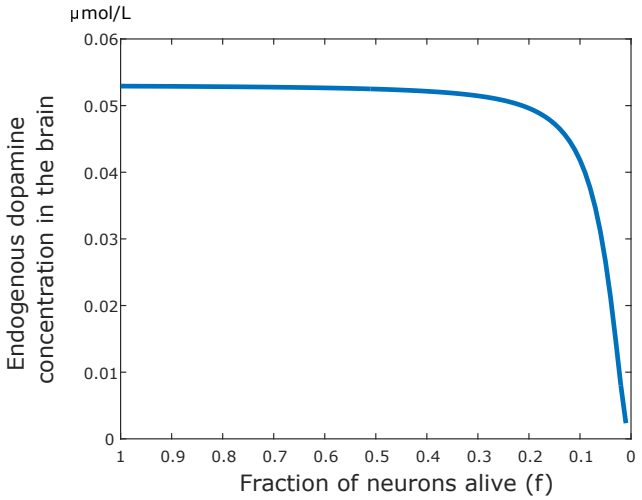

Fig. 7 Endogenous dopamine concentration in the brain as a function of the fraction of neurons alive (f)

3.1.2 Dopamine kinetics model

Parkinson's disease symptoms do not appear until only about 10% to 40% of neurons (represented by the parameter f in the present model) of the substantia nigra remain alive [2,79]. Dopamine concentration does not decrease significantly until approximatively 15% of the neurons are alive [8,10,23]. Before reaching this threshold of denervation, adjustment of the different processes involved in dopamine kinetics allows the dopamine concentration to remain constant. This compensation phenomenon is represented in the model. Indeed, while the fraction of neurons alive f decreases, dopamine concentration does not change until approximatively only 30% subsists. The endogenous concentration of dopamine as a function of the fraction f of neurons alive is simulated using equation 10 and shown in Figure 7. Only endogenous dopamine is considered here so the parameter $I_{DAlevodopa}(t)$ of equation 8 was set to zero.

The decarboxylation of levodopa in the brain will contribute to the increase in dopamine release. The resulting dopaminergic concentration in the synaptic cleft (C_{Dop}) is given by the dopamine kinetics model. It was reported that dopamine concentration increases to 0.17 μmol/L with levodopa medication close to therapeutic dose compared to 0.07 μmol/L without the medication [25]. In [71], dopamine concentrations without medication were on the order of $0.01-0.03$ μmol/L. Similar dopamine concentrations were obtained with the current model, increasing from ~ 0.05 μmol/L in the absence of medication to ~ 0.1 μmol/L with levodopa, in the case where only a 30% fraction of neurons are still alive.

At an early stage of the disease, the buffering capacity of the neurons allows dopamine concentration in the brain to be maintained at a constant level even when levodopa plasma concentration is fluctuating [59]. This buffering

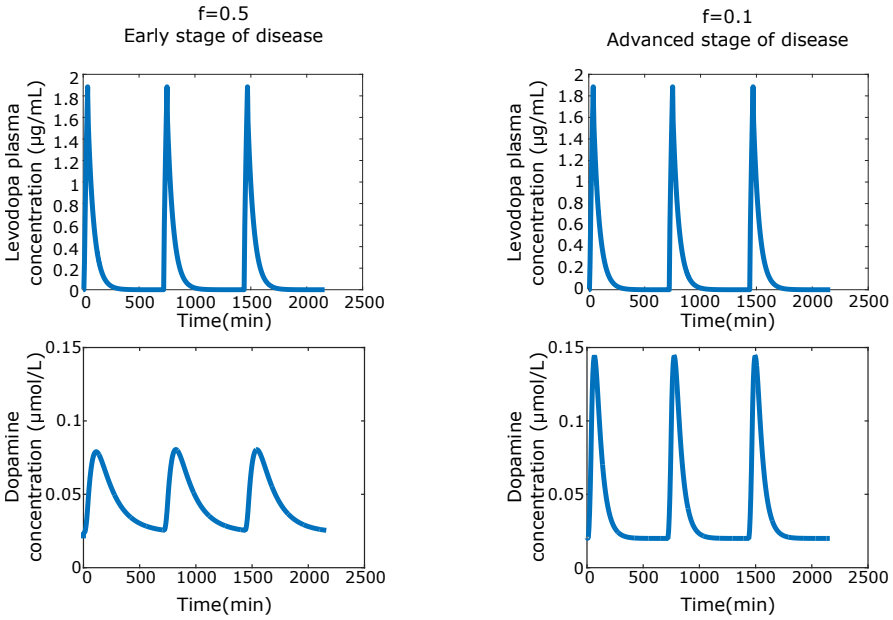

Fig. 8 Levodopa plasma concentration and related dopamine brain concentration in time. Left: Concentrations for early stage of disease with a fraction of neurons alive of 50%; Right: Concentrations for advanced stage of disease with a fraction of neurons alive of 10%.

capacity of the neurons is progressively lost with denervation. Fluctuations in dopamine concentration are then appearing and tend to mimic levodopa plasma concentration. This phenomenon is simulated using the combination of the PK model with the dopamine kinetics model. Figure 8 depicts the plasma concentration of levodopa and the related dopamine concentration in the brain for different fractions of neurons alive. This observed pattern [59] is reproduced here with our model. As seen in Figure 8, basal dopamine concentration is smaller than ~ 0.05 μmol/L. This is due to autoreceptors feedback that decreases dopamine release when levodopa is taken [25]. Autoreceptors are not explicitly modeled in this work, but their influence on dopamine release is represented. Details are found in Supplementary material section S.2. Basal dopamine concentration is also decreased due to denervation, especially in the case of $f = 0.1$.

3.2 Simulation of a patient

Using the whole model, simulations were performed with the set of parameter values given above. The effect of dopamine in the basal ganglia, assigned in [6] to fit the finger tapping data, is simulated here assuming a fraction of neurons alive of 30%, $f = 0.3$. The model allows the plasma concentration, the concentration of levodopa in the brain, the corresponding dopamine concentration in

the brain and the fraction of occupied receptors D1 and D2 to be expressed as a function of time. The fractions of occupied receptors are calculated as follows: Bound receptor$_i/B^i_{max}$ with $i = \{D_1, D_2\}$. The resulting simulations are shown in Figure 9. The patient was simulated using the whole model with $f = 0.3$. With these simulations, the maximal tapping frequency, the levodopa plasma concentration at 50% (EC50) and the baseline tapping were estimated to 175 taps/min, 0.78 $\mu g/mL$ and 118 taps/min, respectively. These values can be visually deduced from Figure 9 (a) and (e) put together. Update E

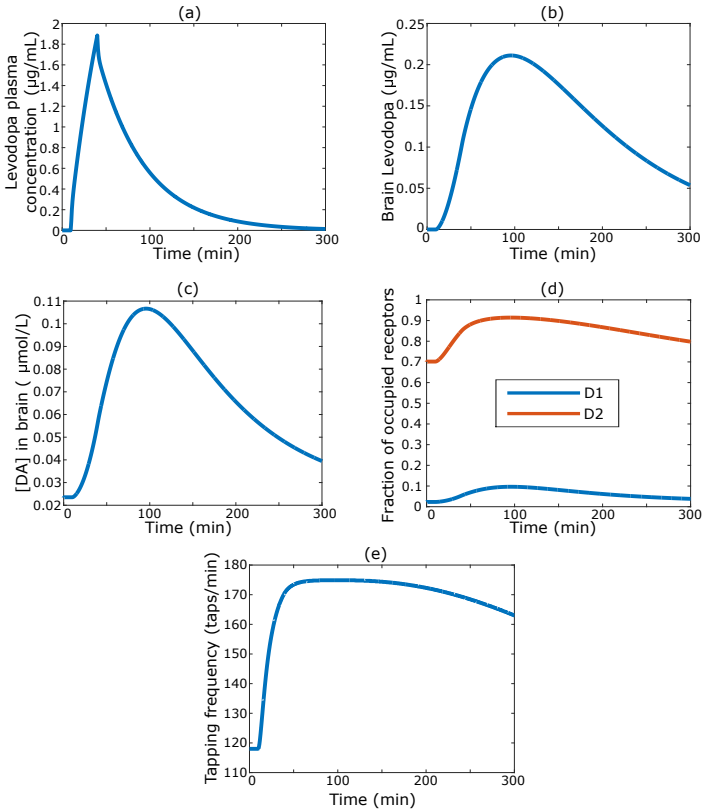

Fig. 9 (a) Levodopa plasma concentration, (b) levodopa brain concentration, (c) dopamine concentration, (d) fraction of occupied dopaminergic receptors D1 and D2 and (e) tapping frequency in time.

3.3 Progression of the disease

At early stages of the disease, levodopa's effect duration extends beyond the duration of the drug in the plasma concentration. As the disease progresses, the onset of levodopa's effect is quicker and the effect duration is shorter. This

phenomenon is well reproduced by the model. Simulations were performed for different fractions of neurons alive (f) in order to represent the progression of the disease. The values of all parameters were kept constant but the fraction f. The results obtained for the tapping frequency over time with the whole model (PK model, dopamine kinetics model and neurocomputational model of basal ganglia) are shown in Figure 10. The fraction of neurons alive was varied between 80% and 5% as observed in experimental studies on animals [47]. A denervation of 5% would represent a score of approximately 73 on the UPDRS3 scale [33]. In Figure 10, baseline frequencies, which are those

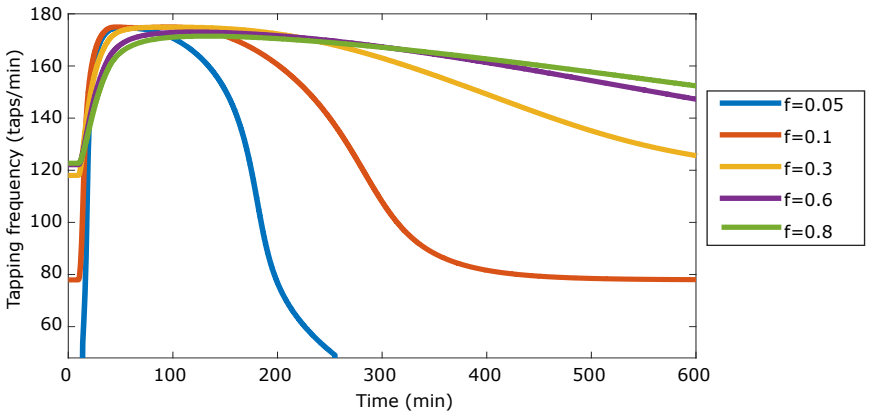

Fig. 10 Tapping frequency in time for different fractions of neurons alive, frequencies before 10 minutes are the basal frequencies before taking the dose

at 10 minutes before taking the dose, decrease with denervation. This is in line with what is reported in the literature [43,57,72]. Our model does not include long duration response of levodopa which could lead to an increase in this baseline tapping frequency [16]. Long duration response could be added in future studies to better capture the effect of levodopa chronic use.

3.4 Receptor's sensitivity analysis

Dopaminergic receptor's density has been shown to change with aging [45] and with nigrostriatal denervation and may be involved in the development of levodopa induced dyskinesia [36,46,63,66]. The maximal density of receptors D_1 and D_2 is represented in the current model by the parameter $B^{D_1}_{max}$ and $B^{D_2}_{max}$ respectively. In an attempt to investigate the impact of a change in each receptor's density, a variation of more or less 40% was applied to each of the parameters $B^{D_1}_{max}$ and $B^{D_2}_{max}$ individually. The resulting tapping frequency as a function of f is given in Figures 11(a) and 12(a). As reported in the literature [32,63], a change in receptor D2 density has a bigger impact on the motor action than that of receptor D1.

Contrary to the maximal receptor density, the affinity of the receptors is not modified with denervation [63]. However, dopamine agonists and antagonists could [12,40,58] modify the affinity of receptors D_1 and D_2, represented here by parameters $k_D^{D_1}$ and $k_D^{D_2}$, respectively. Dopamine receptor agonists are used to delay the starting of levodopa therapy and in advanced stages of Parkinson's disease, they are also used in combination with levodopa [32].

In order to study the impact of each receptor, their affinities were changed independently. A variation of more or less 40% was added to the affinity of receptor D_1 and then of D_2. The tapping frequency as a function of the fraction of neurons alive was computed and the results are shown in Figures 11(b) and 12(b). The tapping frequency is more affected by a modification in receptor D2 affinity. The model predicts a better effectiveness of D2 agonists over D1

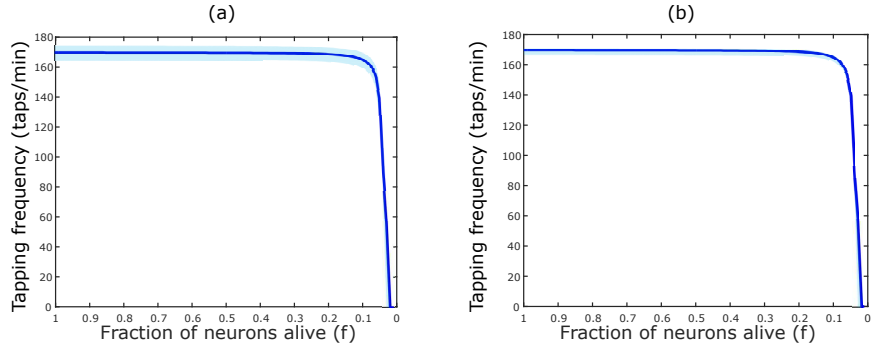

Fig. 11 Tapping frequency at equilibrium without levodopa as a function of the fraction of neurons alive for receptor D1 (a) B_{max}^{D1} ±40% and (b) k_D^{D1} ±40%.

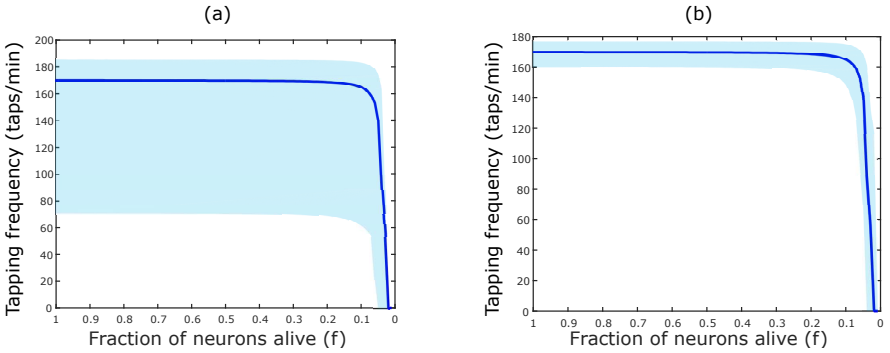

Fig. 12 Tapping frequency at equilibrium without levodopa as a function of the fraction of neurons alive for receptor D2 (a) B_{max}^{D2} ±40% and (b) k_D^{D2} ±40%.

agonists, which confirms the current clinical use.

4 Discussion

The main objective of this study was to develop a mechanistic model that integrates neurodynamics of basal ganglia, dopamine kinetics and levodopa kinetics in order to understand the different mechanisms involved in the modification of levodopa's effect as Parkinson's disease progresses. The relationship between denervation and the more rapid onset and the shorter effect duration of levodopa was investigated.

Three models were combined to represent the important underlying processes. First, a two compartment pharmacokinetic model of levodopa, connected to a third compartment of levodopa's brain concentration was adapted. Then, dopamine kinetics in the striatum was modeled by the inclusion of the main components, namely, release, recapture by DATs and removal. Finally, a neurocomputational model of basal ganglia was used to represent the three neurotransmission pathways and the impact of dopamine on these pathways and on cholinergic interneurons. These models were then connected through scaling or units modification. The involved parameters were derived from animal or human data or fitted to data in previously published studies. Validation was performed with the output of each model to ensure consistency with clinical observations.

We used the full model to produce levodopa's plasma and brain concentrations, dopamine concentrations, fraction of bound receptors and motor activity (finger tapping frequency) in function of time, Figure 9. Disease progression was also investigated by simulating the tapping frequency in time for a same dose of levodopa with different fractions of neurons alive, as shown in Figure 10. We also used the model to illustrate the pulsatile patterns of dopamine, induced by the therapy throughout the disease progression, Figure 8. Disease severity is here given by the fraction f of neurons alive in the substantia nigra. It was shown to be related in a linear way to UPDRS3 score [33]. Few studies analyzed the relation between Hoehn and Yahr scale (H&Y) in Parkinson's disease with UPDRS. In a previous study [69], it was concluded that UPDRS scores for all 4 parts increase significantly with every H&Y stage and also with 5-years increaments of disease duration in the first 15 years of the disease. The fraction f is then somehow also related to H&Y scale. Distribution and elimination from the brain compartment as well as dopamine release, recapture by DATs and removal are the processes affected by the progression of the disease.

The neurocomputational model used in the current study was previously built to simulate the finger tapping task with levodopa administration [6]. We here expanded this model through the addition of dopamine kinetics description. To investigate the impact of the disease progression, expressed here in terms of neurons loss, on the different mechanisms, it was important to detail the dopamine kinetics since nonlinear relationships are involved with denervation.

Additional action channels could be used to represent more complex motor tasks, which can still be addressed with the modeling structure developed here. The neurocomputational model of basal ganglia was previously used with four

action channels [7]. The present model can be applied to study bradykinesia using toe tapping or pronation/supination movements for both hands as a measure of slowness of movements [31]. It could also be used in future studies to investigate different action selection patterns representing dyskinesias and motor fluctuations as in [75].

Previous studies have focused their efforts on understanding Parkinson's disease by developing neurocomputational models of basal ganglia [5,7,6,14, 21,28,37,29,35,50,65,75,78]. Several neurocomputational models of basal ganglia explicitly include the basal ganglia subregions where one to three of the neurotransmission pathways are represented [7,6,14,21,28,37,29,35,50,65,78]. Additional to finger tapping, bradykinesia was evaluated through arm movement [21]. Other symptoms such as handwriting [29], tremor [37] or the impact of learning [5,7,28], reward, punishment [35] and synaptic plasticity [65,75,78] were also considered in several neurocomputational models. As opposed to our model, dopamine kinetics was not explicitly considered in these studies.

The disease progression was also investigated through modeling of dopamine kinetics as an isolated phenomenon per se with [25,60,61] and without [9,26] considering the impact of neuronal death and levodopa intake. The importance of the compensation mechanisms in signaling through dopamine receptors D1 and D2 [26,25], the release and recapture of dopamine [9,60] and the serotoninergic system [61] in dopamine kinetics were previously highlighted. However, the implication of the different processes of dopamine kinetics in the basal ganglia intrinsic function was not part of these studies. It is important to investigate the relation of dopamine and neuronal activity in the basal ganglia for a better understanding of the disease and its medication.

The model developed here is intended to represent a more holistic approach of Parkinson's disease and its therapy, with an attempt to reach a good balance between simplicity and accuracy. We were also concerned by the physiological interpretation of the involved parameters and an appropriate comparison with existing data. The model can be used in the context of two different time scales, one on a scale of hours in order to monitor the effect of the drug following its administration; the other is on a much longer scale with the objective of investigating the progression of the disease. The novelty of this work lies in its mechanistic approach of the drug to clinical effect during the progression of Parkinson's disease.

The model would benefit from the addition of the effect of tonic versus phasic dopamine [26], as well as dopamine release by serotoninergic neurons [61]. A better estimation of the individual weights parameters of the neurocomputational model would help individualize therapeutic predictions by using a customized model to assess the patient's motor activity. A limitation of the model is the non-identifiability of parameters Q_{12} and Q_{21} in the pharmacokinetic model. Since we did not have pharmacokinetic data, we used the parameters values reported in [6]. However, as formulated and with the accessible data, the model of [6] presents a fundamental issue of identifiability (parameters Q_{12} and Q_{21} are not uniquely defined). Scaling was used to connect the dopamine kinetics model to the neurocomputational model of basal

Update C

ganglia in order to maintain the value of synaptic weights originally fitted to patients data. Refitting data with this new model would prevent the need for scaling. We are confident this scaling does not significantly change the output of the model. The ultimate purpose of this modeling exercise is to optimize levodopa's regimen. As dyskinesia is reported as the main side effect of the chronic use of levodopa [75], extension of our model to integrate this motor complication would inform on the evolution towards the thin line that separates levodopa benefits from harm effects throughout the disease.

Indeed, dyskinesias could possibly be delayed by reducing the dose while maintaining the beneficial effect. Different routes of administration of levodopa are tested due to the occurrence of side effects and due to the progression of the disease [4]. In future studies, other pharmacokinetic models (duodenal infusion, oral,..) could be added to the present model to determine not only optimized regimens but also optimized route of administration of levodopa for each patient.

The present model assumes a homogeneous death of neurons in the substantia nigra. However, recent studies [25] showed heterogenous loss of neurons, with the existence of completely void regions. The link between reduction in dopamine and the lost of spatial coherence in innervation is however beyond the scope of our present work. In the present study, the conditions for well-mixed levodopa pharmacokinetics and dopamine kinetics models hold, and this assumption is commonly used in the literature on levodopa pharmacokinetics. Synaptic space with tonic firing has also been shown to be well-mixed [77].

Finally, a sensitivity analysis could be carried out for the herein proposed model with dopamine kinetics in order to determine the most important mechanisms in the onset of symptoms and loss of effect of levodopa. For this, we can draw on a recent work by Ursino et al. [75] which performed a sensitivity analysis of the Go/NoGo pathways, the STN and the cholinergic interneurons.

To conclude, the integrative model developed here was able to reproduce the behaviour of levodopa's effect by representing its most important mechanisms, especially the fact that the therapeutic effect of levodopa start to mimic plasma concentration with the progression of the disease. This quantitative systems approach is a promising step towards the understanding of important mechanisms involved in Parkinson's disease and designing optimal drug regimens.

Acknowledgements F.V.-V. received a scholarship from the Natural Sciences and Engineering Research Council (NSERC), Canada through the PGS-D program. Support was also provided by NSERC -Industrial Chair in Pharmacometrics funded by Novartis, Pfizer and Syneos, as well as FRQNT Projet d'équipe (F.N.).

Conflict of interest

The authors declare that they have no conflict of interest.

References

1. Adamiak, U., Kaldonska, M., Klodowska-Duda, G., Wyska, E., Safranow, K., Bialecka, M., Gawronska-Szklarz, B.: Pharmacokinetic-pharmacodynamic modeling of levodopa in patients with advanced parkinson disease. Clinical neuropharmacology **33**, 135–141 (2010). DOI 10.1097/WNF.0b013e3181d47849
2. Agid, Y.: Parkinson's disease: pathophysiology. Lancet (London, England) **337**, 1321–1324 (1991). DOI 10.1016/0140-6736(91)92989-f
3. Albin, R.L., Young, A.B., Penney, J.B.: The functional anatomy of basal ganglia disorders. Trends in neurosciences **12**, 366–375 (1989)
4. Aquilonius, S.M., Nyholm, D.: Development of new levodopa treatment strategies in parkinson's disease-from bedside to bench to bedside. Upsala journal of medical sciences **122**, 71–77 (2017). DOI 10.1080/03009734.2017.1285374
5. Ashby, F.G., Crossley, M.J.: A computational model of how cholinergic interneurons protect striatal-dependent learning. Journal of Cognitive Neuroscience **23**(6), 1549–1566 (2011). DOI 10.1162/jocn.2010.21523
6. Baston, C., Contin, M., Buonaura, G.C., Cortelli, P., Ursino, M.: A mathematical model of levodopa medication effect on basal ganglia in parkinson's disease: An application to the alternate finger tapping task. Frontiers in Human Neuroscience **10** (2016). DOI 10.3389/fnhum.2016.00280
7. Baston, C., Ursino, M.: A biologically inspired computational model of basal ganglia in action selection. Computational Intelligence and Neuroscience **2015**, 1–24 (2015). DOI 10.1155/2015/187417
8. Bergstrom, B.P., Garris, P.A.: "passive stabilization" of striatal extracellular dopamine across the lesion spectrum encompassing the presymptomatic phase of parkinson's disease: a voltammetric study in the 6-ohda-lesioned rat. Journal of neurochemistry **87**, 1224–1236 (2003). DOI 10.1046/j.1471-4159.2003.02104.x
9. Best, J.A., Nijhout, H.F., Reed, M.C.: Homeostatic mechanisms in dopamine synthesis and release: a mathematical model. Theoretical Biology and Medical Modelling **6**(1) (2009). DOI 10.1186/1742-4682-6-21
10. Bezard, E., Dovero, S., Prunier, C., Ravenscroft, P., Chalon, S., Guilloteau, D., Crossman, A.R., Bioulac, B., Brotchie, J.M., Gross, C.E.: Relationship between the appearance of symptoms and the level of nigrostriatal degeneration in a progressive 1-methyl-4-phenyl-1,2,3,6-tetrahydropyridine-lesioned macaque model of parkinson's disease. The Journal of neuroscience : the official journal of the Society for Neuroscience **21**, 6853–6861 (2001)
11. Black, K.J., Acevedo, H.K., Koller, J.M.: Dopamine buffering capacity imaging: A pharmacodynamic fmri method for staging parkinson disease. Frontiers in Neurology **11**, 370 (2020). DOI 10.3389/fneur.2020.00370. URL https://www.frontiersin.org/article/10.3389/fneur.2020.00370
12. Boileau, I., Guttman, M., Rusjan, P., Adams, J.R., Houle, S., Tong, J., Hornykiewicz, O., Furukawa, Y., Wilson, A.A., Kapur, S., Kish, S.J.: Decreased binding of the d3 dopamine receptor-preferring ligand [11c]-(+)-phno in drug-naive parkinson's disease. Brain : a journal of neurology **132**, 1366–1375 (2009). DOI 10.1093/brain/awn337
13. Budygin, E.A., John, C.E., Mateo, Y., Jones, S.R.: Lack of cocaine effect on dopamine clearance in the core and shell of the nucleus accumbens of dopamine transporter knockout mice. The Journal of neuroscience : the official journal of the Society for Neuroscience **22**, RC222 (2002). DOI 20026389
14. Cavanagh, J.F., Wiecki, T.V., Cohen, M.X., Figueroa, C.M., Samanta, J., Sherman, S.J., Frank, M.J.: Subthalamic nucleus stimulation reverses mediofrontal influence over decision threshold. Nature Neuroscience **14**(11), 1462–1467 (2011). DOI 10.1038/nn.2925
15. Chan, P.L.S., Nutt, J.G., Holford, N.H.G.: Modeling the short- and long-duration responses to exogenous levodopa and to endogenous levodopa production in parkinson's disease. Journal of pharmacokinetics and pharmacodynamics **31**, 243–268 (2004)
16. Chan, P.L.S., Nutt, J.G., Holford, N.H.G.: Pharmacokinetic and pharmacodynamic changes during the first four years of levodopa treatment in parkinson's disease. Journal of pharmacokinetics and pharmacodynamics **32**, 459–484 (2005). DOI 10.1007/s10928-005-0055-x

17. Chou, Y.H., Karlsson, P., Halldin, C., Olsson, H., Farde, L.: A pet study of d(1)-like dopamine receptor ligand binding during altered endogenous dopamine levels in the primate brain. Psychopharmacology **146**, 220–227 (1999). DOI 10.1007/s002130051110
18. Contin, M., Riva, R., Martinelli, P., Albani, F., Avoni, P., Baruzzi, A.: Levodopa therapy monitoring in patients with parkinson disease: a kinetic-dynamic approach. Therapeutic drug monitoring **23**, 621–629 (2001)
19. Cotzias, G.C., Van Woert, M.H., Schiffer, L.M.: Aromatic amino acids and modification of parkinsonism. The New England journal of medicine **276**, 374–379 (1967). DOI 10.1056/NEJM196702162760703
20. Crossman, A.R., Clarke, C.E., Boyce, S., Robertson, R.G., Sambrook, M.A.: Mptp-induced parkinsonism in the monkey: neurochemical pathology, complications of treatment and pathophysiological mechanisms. The Canadian journal of neurological sciences. Le journal canadien des sciences neurologiques **14**, 428–435 (1987). DOI 10.1017/s0317167100037859
21. Cutsuridis, V., Perantonis, S.: A neural network model of parkinson's disease bradykinesia. Neural networks : the official journal of the International Neural Network Society **19**, 354–374 (2006). DOI 10.1016/j.neunet.2005.08.016
22. DeLong, M.R.: Primate models of movement disorders of basal ganglia origin. Trends in neurosciences **13**, 281–285 (1990)
23. Dentresangle, C., Le Cavorsin, M., Savasta, M., Leviel, V.: Increased extracellular da and normal evoked da release in the rat striatum after a partial lesion of the substantia nigra. Brain research **893**, 178–185 (2001). DOI 10.1016/s0006-8993(00)03311-4
24. Dietz, M., Harder, S., Graff, J., Knig, G., Vontobel, P., Leenders, K.L., Baas, H.: Levodopa pharmacokinetic-pharmacodynamic modeling and 6-[18f]levodopa positron emission tomography in patients with parkinson's disease. Clinical pharmacology and therapeutics **70**, 33–41 (2001). DOI 10.1067/mcp.2001.116328
25. Dreyer, J.K.: Three mechanisms by which striatal denervation causes breakdown of dopamine signaling. Journal of Neuroscience **34**(37), 12444–12456 (2014). DOI 10.1523/jneurosci.1458-14.2014
26. Dreyer, J.K., Herrik, K.F., Berg, R.W., Hounsgaard, J.D.: Influence of phasic and tonic dopamine release on receptor activation. Journal of Neuroscience **30**(42), 14273–14283 (2010). DOI 10.1523/JNEUROSCI.1894-10.2010. URL https://www.jneurosci.org/content/30/42/14273
27. Fabbrini, G., Juncos, J., Mouradian, M.M., Serrati, C., Chase, T.N.: Levodopa pharmacokinetic mechanisms and motor fluctuations in parkinson's disease. Annals of neurology **21**, 370–376 (1987). DOI 10.1002/ana.410210409
28. Frank, M.J.: Dynamic dopamine modulation in the basal ganglia: A neurocomputational account of cognitive deficits in medicated and nonmedicated parkinsonism. Journal of Cognitive Neuroscience **17**(1), 51–72 (2005). DOI 10.1162/0898929052880093. URL https://doi.org/10.1162/0898929052880093
29. Gangadhar, G., Joseph, D., Srinivasan, A.V., Subramanian, D., Shivakeshavan, R.G., Shobana, N., Chakravarthy, V.S.: A computational model of parkinsonian handwriting that highlights the role of the indirect pathway in the basal ganglia. Human movement science **28**, 602–618 (2009). DOI 10.1016/j.humov.2009.07.008
30. Gerfen, C.R., Engber, T.M., Mahan, L.C., Susel, Z., Chase, T.N., Monsma, F.J., Sibley, D.R.: D1 and d2 dopamine receptor-regulated gene expression of striatonigral and striatopallidal neurons. Science (New York, N.Y.) **250**, 1429–1432 (1990). DOI 10.1126/science.2147780
31. Goetz, C.G., Tilley, B.C., Shaftman, S.R., Stebbins, G.T., Fahn, S., Martinez-Martin, P., Poewe, W., Sampaio, C., Stern, M.B., Dodel, R., Dubois, B., Holloway, R., Jankovic, J., Kulisevsky, J., Lang, A.E., Lees, A., Leurgans, S., LeWitt, P.A., Nyenhuis, D., Olanow, C.W., Rascol, O., Schrag, A., Teresi, J.A., van Hilten, J.J., LaPelle, N., Force, M.D.S.U.R.T.: Movement disorder society-sponsored revision of the unified parkinson's disease rating scale (mds-updrs): scale presentation and clinimetric testing results. Movement disorders : official journal of the Movement Disorder Society **23**, 2129–2170 (2008). DOI 10.1002/mds.22340
32. Gomez, G., Escande, M.V., Suarez, L.M., Rela, L., Belforte, J.E., Moratalla, R., Murer, M.G., Gershanik, O.S., Taravini, I.R.E.: Changes in dendritic spine density and in-

hibitory perisomatic connectivity onto medium spiny neurons in l-dopa-induced dyskinesia. Molecular neurobiology **56**, 6261–6275 (2019). DOI 10.1007/s12035-019-1515-4
33. Greffard, S., Verny, M., Bonnet, A.M., Beinis, J.Y., Gallinari, C., Meaume, S., Piette, F., Hauw, J.J., Duyckaerts, C.: Motor score of the unified parkinson disease rating scale as a good predictor of lewy body–associated neuronal loss in the substantia nigra. Archives of Neurology **63**(4), 584 (2006). DOI 10.1001/archneur.63.4.584
34. Group, P.S.: Dopamine transporter brain imaging to assess the effects of pramipexole vs levodopa on parkinson disease progression. JAMA **287**, 1653–1661 (2002). DOI 10.1001/jama.287.13.1653
35. Guthrie, M., Myers, C.E., Gluck, M.A.: A neurocomputational model of tonic and phasic dopamine in action selection: a comparison with cognitive deficits in parkinson's disease. Behavioural brain research **200**, 48–59 (2009). DOI 10.1016/j.bbr.2008.12.036
36. Guttman, M., Seeman, P.: L-dopa reverses the elevated density of d2 dopamine receptors in parkinson's diseased striatum. Journal of neural transmission **64**, 93–103 (1985). DOI 10.1007/bf01245971
37. Haeri, M., Sarbaz, Y., Gharibzadeh, S.: Modeling the parkinson's tremor and its treatments. Journal of Theoretical Biology **236**(3), 311–322 (2005). DOI 10.1016/j.jtbi.2005.03.014
38. Harder, S., Baas, H.: Concentration-response relationship of levodopa in patients at different stages of parkinson's disease. Clinical pharmacology and therapeutics **64**, 183–191 (1998). DOI 10.1016/S0009-9236(98)90152-7
39. Hille, B.: G protein-coupled mechanisms and nervous signaling. Neuron **9**(2), 187–195 (1992). DOI 10.1016/0896-6273(92)90158-a
40. Hisahara, S., Shimohama, S.: Dopamine receptors and parkinson's disease. International journal of medicinal chemistry **2011**, 403039 (2011). DOI 10.1155/2011/403039
41. Holford, N., Nutt, J.G.: Disease progression, drug action and parkinson's disease: why time cannot be ignored. European journal of clinical pharmacology **64**, 207–216 (2008). DOI 10.1007/s00228-007-0427-9
42. Holford, N.H.G., Chan, P.L.S., Nutt, J.G., Kieburtz, K., Shoulson, I., Group, P.S.: Disease progression and pharmacodynamics in parkinson disease - evidence for functional protection with levodopa and other treatments. Journal of pharmacokinetics and pharmacodynamics **33**, 281–311 (2006). DOI 10.1007/s10928-006-9012-6
43. Homann, C.N., Suppan, K., Wenzel, K., Giovannoni, G., Ivanic, G., Horner, S., Ott, E., Hartung, H.P.: The bradykinesia akinesia incoordination test (brain test), an objective and user-friendly means to evaluate patients with parkinsonism. Movement disorders : official journal of the Movement Disorder Society **15**, 641–647 (2000)
44. Hunger, L., Kumar, A., Schmidt, R.: Abundance compensates kinetics: Similar effect of dopamine signals on d1 and d2 receptor populations. Journal of Neuroscience **40**(14), 2868–2881 (2020). DOI 10.1523/JNEUROSCI.1951-19.2019. URL https://www.jneurosci.org/content/40/14/2868
45. Kuwabara, H., McCaul, M.E., Wand, G.S., Earley, C.J., Allen, R.P., Weerts, E.M., Dannals, R.F., Wong, D.F.: Dissociative changes in the bmax and kd of dopamine d2/d3 receptors with aging observed in functional subdivisions of the striatum: a revisit with an improved data analysis method. Journal of nuclear medicine : official publication, Society of Nuclear Medicine **53**, 805–812 (2012). DOI 10.2967/jnumed.111.098186
46. Lee, T., Seeman, P., Rajput, A., Farley, I.J., Hornykiewicz, O.: Receptor basis for dopaminergic supersensitivity in parkinson's disease. Nature **273**, 59–61 (1978). DOI 10.1038/273059a0
47. Lopez, A., Muoz, A., Guerra, M.J., Labandeira-Garcia, J.L.: Mechanisms of the effects of exogenous levodopa on the dopamine-denervated striatum. Neuroscience **103**, 639–651 (2001). DOI 10.1016/s0306-4522(00)00588-1
48. May, T.: Striatal dopamine d1-like receptors have higher affinity for dopamine in ethanol-treated rats. European Journal of Pharmacology **215**(2-3), 313–316 (1992). DOI 10.1016/0014-2999(92)90047-8
49. Mink, J.W.: The basal ganglia: Focused selection and inhibition of competing motor programs. Progress in Neurobiology **50**(4), 381 – 425 (1996). DOI https://doi.org/10.1016/S0301-0082(96)00042-1. URL http://www.sciencedirect.com/science/article/pii/S0301008296000421

50. Moustafa, A.A., Gluck, M.A.: A neurocomputational model of dopamine and prefrontal–striatal interactions during multicue category learning by parkinson patients. Journal of Cognitive Neuroscience **23**(1), 151–167 (2011). DOI 10.1162/jocn.2010.21420
51. Neve, K.A., Neve, R.L.: Molecular Biology of Dopamine Receptors, pp. 27–76. Humana Press, Totowa, NJ (1997). DOI 10.1007/978-1-4757-2635-0 2. URL https://doi.org/10.1007/978-1-4757-2635-0 2
52. Nord, M., Zsigmond, P., Kullman, A., Dizdar, N.: Levodopa pharmacokinetics in brain after both oral and intravenous levodopa in one patient with advanced parkinson's disease. Advances in Parkinson's Disease **06**(02), 52–66 (2017). DOI 10.4236/apd.2017.62006
53. Nutt, J.G., Holford, N.H.: The response to levodopa in parkinson's disease: imposing pharmacological law and order. Annals of neurology **39**, 561–573 (1996). DOI 10.1002/ana.410390504
54. Nutt, J.G., Woodward, W.R., Carter, J.H., Gancher, S.T.: Effect of long-term therapy on the pharmacodynamics of levodopa. relation to on-off phenomenon. Archives of neurology **49**, 1123–1130 (1992). DOI 10.1001/archneur.1992.00530350037016
55. Olanow, C.W., Agid, Y., Mizuno, Y., Albanese, A., Bonuccelli, U., Bonucelli, U., Damier, P., De Yebenes, J., Gershanik, O., Guttman, M., Grandas, F., Hallett, M., Hornykiewicz, O., Jenner, P., Katzenschlager, R., Langston, W.J., LeWitt, P., Melamed, E., Mena, M.A., Michel, P.P., Mytilineou, C., Obeso, J.A., Poewe, W., Quinn, N., Raisman-Vozari, R., Rajput, A.H., Rascol, O., Sampaio, C., Stocchi, F.: Levodopa in the treatment of parkinson's disease: current controversies. Movement disorders : official journal of the Movement Disorder Society **19**, 997–1005 (2004). DOI 10.1002/mds.20243
56. Olanow, W., Schapira, A.H., Rascol, O.: Continuous dopamine-receptor stimulation in early parkinson's disease. Trends in neurosciences **23**, S117–S126 (2000). DOI 10.1016/s1471-1931(00)00030-6
57. Pal, P.K., Lee, C.S., Samii, A., Schulzer, M., Stoessl, A.J., Mak, E.K., Wudel, J., Dobko, T., Tsui, J.K.: Alternating two finger tapping with contralateral activation is an objective measure of clinical severity in parkinson's disease and correlates with pet. Parkinsonism & related disorders **7**, 305–309 (2001). DOI 10.1016/s1353-8020(00)00048-1
58. Payer, D.E., Guttman, M., Kish, S.J., Tong, J., Adams, J.R., Rusjan, P., Houle, S., Furukawa, Y., Wilson, A.A., Boileau, I.: D3 dopamine receptor-preferring [11c]phno pet imaging in parkinson patients with dyskinesia. Neurology **86**, 224–230 (2016). DOI 10.1212/WNL.0000000000002285
59. Poewe, W., Antonini, A., Zijlmans, J.C., Burkhard, P.R., Vingerhoets, F.: Levodopa in the treatment of parkinson's disease: an old drug still going strong. Clinical interventions in aging **5**, 229–238 (2010)
60. Reed, M.C., Best, J., Nijhout, H.F.: Passive and active stabilization of dopamine in the striatum. Bioscience Hypotheses **2**(4), 240 – 244 (2009). DOI https://doi.org/10.1016/j.bihy.2009.03.008. URL http://www.sciencedirect.com/science/article/pii/S1756239209000494
61. Reed, M.C., Nijhout, H.F., Best, J.A.: Mathematical insights into the effects of levodopa. Frontiers in integrative neuroscience **6**, 21 (2012). DOI 10.3389/fnint.2012.00021
62. Richfield, E., Penney, J., Young, A.: Anatomical and affinity state comparisons between dopamine d1 and d2 receptors in the rat central nervous system. Neuroscience **30**(3), 767–777 (1989). DOI 10.1016/0306-4522(89)90168-1
63. Rinne, J.O., Laihinen, A., Ruottinen, H., Ruotsalainen, U., Ngren, K., Lehikoinen, P., Oikonen, V., Rinne, U.K.: Increased density of dopamine d2 receptors in the putamen, but not in the caudate nucleus in early parkinson's disease: a pet study with [11c]raclopride. Journal of the neurological sciences **132**, 156–161 (1995). DOI 10.1016/0022-510x(95)00137-q
64. Salamon, A., Zádori, D., Szpisjak, L., Klivényi, P., Vécsei, L.: Neuroprotection in parkinson's disease: facts and hopes. Journal of Neural Transmission **127**(5), 821–829 (2019). DOI 10.1007/s00702-019-02115-8
65. Schroll, H., Vitay, J., Hamker, F.H.: Working memory and response selection: a computational account of interactions among cortico-basalganglio-thalamic loops. Neural networks : the official journal of the International Neural Network Society **26**, 59–74 (2012). DOI 10.1016/j.neunet.2011.10.008

66. Seeman, P., Niznik, H.B.: Dopamine receptors and transporters in parkinson's disease and schizophrenia. FASEB journal : official publication of the Federation of American Societies for Experimental Biology **4**, 2737–2744 (1990). DOI 10.1096/fasebj.4.10.2197154
67. Senek, M., Nyholm, D., Nielsen, E.I.: Population pharmacokinetics of levodopa/carbidopa microtablets in healthy subjects and parkinson's disease patients. European journal of clinical pharmacology **74**, 1299–1307 (2018). DOI 10.1007/s00228-018-2497-2
68. Sharma, S., Moon, C.S., Khogali, A., Haidous, A., Chabenne, A., Ojo, C., Jelebinkov, M., Kurdi, Y., Ebadi, M.: Biomarkers in parkinson's disease (recent update). Neurochemistry international **63**, 201–229 (2013). DOI 10.1016/j.neuint.2013.06.005
69. Skorvanek, M., Martinez-Martin, P., Kovacs, N., Rodriguez-Violante, M., Corvol, J.C., Taba, P., Seppi, K., Levin, O., Schrag, A., Foltynie, T., Alvarez-Sanchez, M., Arakaki, T., Aschermann, Z., Aviles-Olmos, I., Benchetrit, E., Benoit, C., Bergareche-Yarza, A., Cervantes-Arriaga, A., Chade, A., Cormier, F., Datieva, V., Gallagher, D.A., Garretto, N., Gdovinova, Z., Gershanik, O., Grofik, M., Han, V., Huang, J., Kadastik-Eerme, L., Kurtis, M.M., Mangone, G., Martinez-Castrillo, J.C., Mendoza-Rodriguez, A., Minar, M., Moore, H.P., Muldmaa, M., Mueller, C., Pinter, B., Poewe, W., Rallmann, K., Reiter, E., Rodriguez-Blazquez, C., Singer, C., Tilley, B.C., Valkovic, P., Goetz, C.G., Stebbins, G.T.: Differences in mds-updrs scores based on hoehn and yahr stage and disease duration. Movement disorders clinical practice **4**, 536–544 (2017). DOI 10.1002/mdc3.12476
70. Smith, L.A., Jackson, M.J., Hansard, M.J., Maratos, E., Jenner, P.: Effect of pulsatile administration of levodopa on dyskinesia induction in drug-nave mptp-treated common marmosets: effect of dose, frequency of administration, and brain exposure. Movement disorders : official journal of the Movement Disorder Society **18**, 487–495 (2003). DOI 10.1002/mds.10394
71. Sulzer, D., Cragg, S.J., Rice, M.E.: Striatal dopamine neurotransmission: Regulation of release and uptake. Basal Ganglia **6**(3), 123–148 (2016). DOI 10.1016/j.baga.2016.02.001
72. Taylor Tavares, A.L., Jefferis, G.S.X.E., Koop, M., Hill, B.C., Hastie, T., Heit, G., Bronte-Stewart, H.M.: Quantitative measurements of alternating finger tapping in parkinson's disease correlate with updrs motor disability and reveal the improvement in fine motor control from medication and deep brain stimulation. Movement disorders : official journal of the Movement Disorder Society **20**, 1286–1298 (2005). DOI 10.1002/mds.20556
73. Thanvi, B.R., Lo, T.C.N.: Long term motor complications of levodopa: clinical features, mechanisms, and management strategies. Postgraduate Medical Journal **80**(946), 452–458 (2004). DOI 10.1136/pgmj.2003.013912. URL https://pmj.bmj.com/content/80/946/452
74. Triggs, E.J., Charles, B.G., Contin, M., Martinelli, P., Cortelli, P., Riva, R., Albani, F., Baruzzi, A.: Population pharmacokinetics and pharmacodynamics of oral levodopa in parkinsonian patients. European journal of clinical pharmacology **51**, 59–67 (1996). DOI 10.1007/s002280050161
75. Ursino, M., Baston, C.: Aberrant learning in parkinson's disease: A neurocomputational study on bradykinesia. The European journal of neuroscience **47**, 1563–1582 (2018). DOI 10.1111/ejn.13960
76. Ursino, M., Magosso, E., Lopane, G., Calandra-Buonaura, G., Cortelli, P., Contin, M.: Mathematical modeling and parameter estimation of levodopa motor response in patients with parkinson disease. PLOS ONE **15**(3), 1–20 (2020). DOI 10.1371/journal.pone.0229729. URL https://doi.org/10.1371/journal.pone.0229729
77. Venton, B.J., Zhang, H., Garris, P.A., Phillips, P.E.M., Sulzer, D., Wightman, R.M.: Real-time decoding of dopamine concentration changes in the caudate-putamen during tonic and phasic firing. Journal of neurochemistry **87**, 1284–1295 (2003). DOI 10.1046/j.1471-4159.2003.02109.x
78. Wiecki, T.V., Frank, M.J.: Neurocomputational models of motor and cognitive deficits in parkinson's disease. Progress in brain research **183**, 275–297 (2010). DOI 10.1016/S0079-6123(10)83014-6

79. Zigmond, M.J., Abercrombie, E.D., Berger, T.W., Grace, A.A., Stricker, E.M.: Compensations after lesions of central dopaminergic neurons: some clinical and basic implications. Trends in neurosciences **13**, 290–296 (1990)